3D Numerical Simulations of Eruption Clouds: A Case Study of the 2011 Shinmoe-dake Eruptions

Project Representative
Takehiro Koyaguchi Earthquake Research Institute, The University of Tokyo

Authors
Yujiro Suzuki Earthquake Research Institute, The University of Tokyo
Takehiro Koyaguchi Earthquake Research Institute, The University of Tokyo

We developed a new three-dimensional (3D) numerical model that calculates eruption cloud dynamics and the wind-borne transport of volcanic ash in order to simulate the formation of volcanic plumes and the distribution of ash fall during the 2011 eruptions of the Kirishima-Shinmoe-dake volcano, Japan. The present model quantitatively reproduces the relationship between the eruption conditions (e.g., magma discharge rate) and field observations, such as plume height and ash fall area. Simulation results indicate that, when wind is present, the plume is strongly bent-over by the wind and develops a horizontally-moving cloud whose height is lower than the case when wind is absent. As the cloud develops, the coarse particles accumulate at the bottom of the horizontally-moving cloud. Subsequently, these particles separate from the cloud and are transported by the atmospheric wind. As the particle size increases, their release height decreases. These sorting processes depend on the wind profile. Our results show that the distributions of fall deposits of the 2011 Shinmoe-dake eruption were controlled not only by the wind direction at the level of the horizontally moving cloud, but also by wind directions at low altitudes.

Keywords: volcanic eruption, eruption column, ash dispersal, turbulent mixing, volcanic hazard

1. Introduction

Explosive eruptions are characterized by the formation of buoyant plumes and widespread dispersal of volcanic ash. During such eruptions, a mixture of solid pyroclasts (volcanic ash) and volcanic gas is ejected from vents into the atmosphere. The ejected material (i.e., the mixture of solid pyroclasts and volcanic gas) generally has an initial density several times higher than that of the atmosphere, since it is composed of more than 90 wt% solid pyroclasts. As the ejected material entrains ambient air, expansion of this air during mixing with the hot pyroclasts drastically decreases the density of the mixture, so that it becomes less dense than the surrounding atmosphere. This results in the development of a buoyant volcanic plume.

Volcanic plume height is one of the key observable quantities to estimate eruption conditions, including eruption intensity (i.e., magma discharge rate). Eruption column dynamics are controlled mainly by the balance between thermal energy ejected from the vent and the work done during transportation of the cloud (i.e., ejected material plus entrained air) through atmospheric stratification. This means that when magma properties (i.e., temperature, volatile content, and heat capacity) are fixed, plume height is dependent on the efficiency of turbulent mixing, the magma discharge rate and atmospheric conditions [e.g., 1, 2].

The flow patterns of a volcanic plume are also strongly dependent on whether plume vertical velocities are faster or slower than wind speeds [3]. Plume trajectories are not wind-affected at high eruption intensities and/or under weak wind speeds. The vertically rising plume spreads horizontally as an umbrella cloud at the level where cloud density is equal to that of the atmosphere, termed the neutral buoyancy level (NBL) [2]. In contrast, if eruption intensity is weak and/or wind speeds are high, volcanic plumes are highly wind-distorted, leading to a bent-over trajectory, and the deposition of volcanic ash at significant distances from the vent. Bursik [4] proposed a theoretical model of bent-over plume, and suggested that wind enhances the efficiency of turbulent mixing, leading to a decrease in plume height. However, the effects of wind on turbulent mixing efficiency and plume height are not quantitatively understood.

In the first stage of the 2011 Kirishima-Shinmoe-dake volcano eruptions in Japan, three volcanic plumes developed; they were strongly affected and distorted by a westerly wind with volcanic ash transported toward the southeast. Weather radar echo measurements indicated that these plumes reached heights of 6.5-8.5 km above sea level (asl) [5]. Kozono et al. [6] pointed out that these plume heights were significantly lower than those predicted by a simple plume height model for the observed magma discharge rate (~11 km). This implies that environmental winds enhance turbulent mixing and cause a

decrease in plume height, as was suggested by Bursik [4]. Here, we present a new three-dimensional (3D) numerical model of bent-over plumes in order to confirm this hypothesis. We also attempt to reproduce the distribution of fall deposits for the 2011 Shinmoe-dake eruptions.

2. Numerical model

Our numerical model is designed to simulate the behavior of a mixture of solid pyroclasts and volcanic gas during explosive volcanic eruption, using a combination of a pseudo-gas model for fluid motion and a Lagrangian model for particle motion. During fluid dynamics calculations, we ignore the separation of solid pyroclasts from the eruption cloud, treating an eruption cloud as a single gas with a density calculated using a mixing ratio between ejected material and entrained air. The fluid dynamics model solves a set of partial differential equations that describe the conservation of mass, momentum, and energy, and constitutive equations describing the thermodynamic state of the mixture of pyroclasts, volcanic gas, and air. These equations are solved numerically by a general scheme for compressible flow. Details of the numerical procedures used in this study are described in Suzuki et al. [7]. For the calculations of particle motion, our model employs Lagrangian marker particles of ideal sphere.

In our Lagrangian model, the density of particles is assumed to be 1000 kg m^{-3}, and 200 marker particles are ejected from the vent every 10 sec at the same velocity as the pseudo-gas. Particle grain sizes are randomly selected within a range of 0.0625 to 64 mm, with a terminal velocity for individual particles (V_t) determined for three ranges of particle Reynolds numbers (Re) as follows:

$$\begin{aligned} V_t &= (3.1 g\sigma d/\rho_a)^{1/2} && (\mathrm{Re} > 500) \\ V_t &= \mathrm{d}\,(4g^2\sigma^2/225\mu\rho_a)^{1/3} && (6 < \mathrm{Re} < 500) \\ V_t &= g\sigma d^2/18\mu && (\mathrm{Re} < 6) \end{aligned} \quad (1)$$

where g is the gravitational body force per unit mass, σ is the particle density, d is the particle diameter, ρ_a is atmospheric density, and μ is the dynamic viscosity of air [e.g., 8]. Particle Reynolds numbers are defined as:

$$\mathrm{Re} = \sigma d \Delta v/\mu, \quad (2)$$

where Δv is the vertical component of relative velocity between the particle and ambient fluid (i.e., mixture of ejected pseudo-gas and air). The terminal velocity (V_t) is added to the vertical velocity of fluid motion at every time step, until the marker particle ceases its motion and settles as sediment when they reach the ground surface.

Calculations were performed in a 3D domain with a non-uniform grid. A computational domain extends 13 km vertically (Z-direction) and 24 km × 2 km horizontally (X- and Y-directions, respectively). From a circular vent on the ground, the mixture of solid pyroclasts and volcanic gas is ejected in a stratified atmosphere. The boundaries are located 2 km north, 10 km south, 1 km west, and 23 km east from the volcanic vent center, which is at 1400 m asl. A free-slip condition is applied at the ground boundary for ejected material and air velocities, with mass, momentum, and energy fluxes at the upper and other boundaries of the computational domain assumed to be continuous; these boundary conditions correspond to free outflow and inflow for these quantities. Grid sizes were set to be smaller than $D_0/16$ near the vent, where D_0 is the vent diameter, and to increase at a constant rate (by a factor of 1.02) with distance from the vent up to $D_0/2$, such that the grid size is small enough to resolve turbulent flow at locations far from the vent [cf. 9].

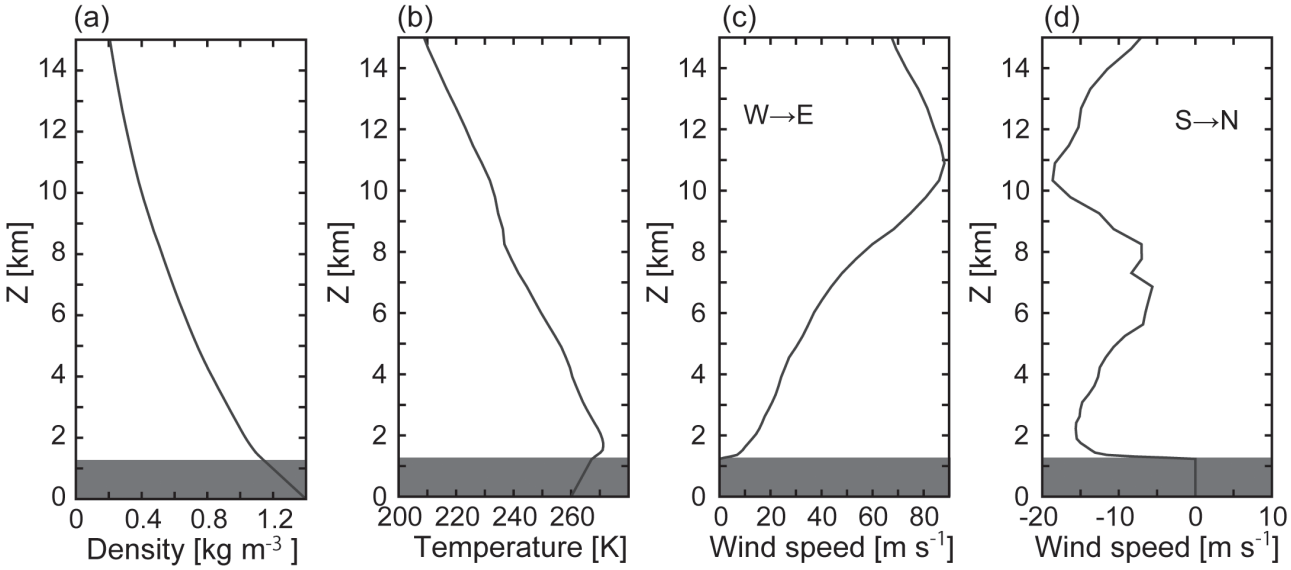

Fig. 1 Initial atmospheric conditions used during simulations: (a) density, (b) temperature, (c) wind speed from west to east, and (d) wind speed from south to north. These profiles were provided by JMANHM model [10].

3. Simulation input parameters

Shinmoe-dake volcano, located in Kyushu, Japan, produced several sustained explosive eruptions between January 26 and 27 in 2011; see Kozono et al. [6] for a more detailed description of these eruptions. The atmospheric conditions at the volcano during the eruption were calculated using the Japan Meteorological Agency's Non-Hydrostatic Model (JMANHM) [10]. This model provides vertical atmospheric density, pressure, temperature, and wind velocity profiles (Fig. 1), indicating that temperature decreased linearly with height (Fig. 1b), with northwesterly winds dominating near the vent (Fig. 1c and 1d). The speed of this westerly wind increased with height, reaching 80 m s^{-1} at 11 km asl. (Fig. 1c). In the simulations presented here, initial atmospheric conditions are given as a function of height (Z) using these vertical profiles, and are assumed to be horizontally uniform at each height, with vertical wind velocity assumed to be zero.

Magmatic properties (i.e., volatile content and magma temperature) were estimated from petrological data, with Suzuki et al. [11] documenting that volatile content (H_2O) ranges from 3 to 5 wt% with magma temperatures around 1273 K. On the basis of these data, the volatile content n_{g0} and magma temperature T_0 in the simulations presented here are set to be 3 wt% and 1273 K, respectively.

Magma discharge rates were precisely estimated using a combined geodetic and satellite observation-based method [6]. A combination of geodetic volume change and lava effusion volume enabled an estimation of the magma discharge rate during the sub-Plinian events, at 450-741 m^3s^{-1}, corresponding to 1.13-1.85x10^6 kg s^{-1}. Here, we assume that the magma discharge rate was 1.5x10^6 kg s^{-1}.

In general, the pressure of a gas-pyroclast mixture at the vent deviates from atmospheric pressure during explosive eruptions, with the mixture accelerated and/or decelerated during decompression and/or compression immediately above the vent [e.g., 12]. For simplicity, we assume that the pressure at the vent is equal to atmospheric pressure, as the pressure of the mixture is considered to approach atmospheric values at a short distance from the vent (5-20 vent radii). This assumption means that the initial density of the ejected material ρ_0 is given as a function of T_0 and n_{g0}. In this study, the exit velocity w_0 is tentatively assumed to be the sound velocity of the mixture (134 m s^{-1}). When the magma discharge rate MDR, mixture density ρ_0, and exit velocity w_0 are given, the vent diameter D_0 is calculated from the relationship as:

$$MDR = \pi\rho_0 w_0 (D_0/2)^2. \quad (3)$$

4. Simulation results

Our simulation successfully reproduced a wind-distorted volcanic plume (Fig. 2). At 480 sec after the eruption, a distal horizontally moving cloud develops at 6-8 km asl (L > 6 km, where L is horizontal distance from the vent), whereas a bent-over plume develops proximal to the vent (L < 6 km; Fig. 2a and 2b). A gas-pyroclast mixture is ejected from the vent with a higher density (5.74 kg m^{-3}) and a higher temperature (1273 K) than the density (1.11 kg m^{-3}) and temperature (270 K) of the atmosphere at ground level (Fig. 2c and 2d). As the cloud rises, it entrains ambient air to decrease the mixture density and to increase cloud buoyancy (Fig. 2c). Temperatures in the rising plume remain higher than the atmospheric temperature (Fig. 2d). When the cloud moves horizontally at a height of 6-8 km, the mass fraction of the ejected material decreases to < 0.05 because of air entrainment (Fig. 2b). In this horizontally moving cloud, the density and temperature of the cloud become almost equal to those of the atmosphere at the same level. The simulated plume height is quantitatively consistent with the plume heights observed by the weather radar echo measurements (6.5-8.5 km asl) [5].

Our simulations also reproduce particle separation and sedimentation from the volcanic plume (Fig. 3). The marker particles ejected from the vent at the same velocity as the pseudo-gas are carried upward by turbulent flow, and leave from the cloud because their density is higher than that of the gas phases. Fine particles (shown by red points in Fig. 3a) are transported to the top of the plume, drift toward the east-southeast in the horizontally moving cloud, and spread toward wind direction gradually in distance. In contrast, coarse particles (blue points) leave from the volcanic plume and fall to the ground near the vent. Medium-sized particles (yellow and green points) are transitional between the fine and coarse particles, and go to higher level than the coarse particles, but not to the top of the plume. Because the northwesterly wind predominates at low altitudes (Fig. 1c and 1d), the particles left from the cloud drift toward the southeast (Fig. 3c). As a consequence, the dispersal axis of the main fall deposit extends toward the southeast (Fig. 3d). These simulated directions of the horizontally moving cloud and the dispersal axis of the fall deposit agree well with the field observations (dashed curves in Fig. 3d) [13]. The above results suggest that the distribution of fall deposits is controlled not only by the wind direction at the level of the horizontally moving cloud, but also by wind directions at low altitudes, whereas the direction of the horizontally moving cloud is mainly governed by the wind direction at high altitudes.

5. Concluding remarks

We developed a 3D numerical model of volcanic plumes in wind fields to simulate the behavior of volcanic plumes during the 2011 Shinmoe-dake eruptions. The simulation results agree well with the height and shape of the plume observed in satellite images and weather radar echo measurements. Our simulations also suggest that the fallout from the eruption cloud was strongly controlled by low-altitude winds below the eruption cloud. Because of this wind effect, the dispersal axis of the fall deposits of the 2011 Shinmoe-dake eruptions extended to the

southeast, whereas the eruption cloud drifted toward the east-southeast.

Although our present model successfully reproduces the main features of the eruption cloud and the fall deposits during the 2011 Shinmoe-dake eruptions, it fails to simulate some detailed features of fall deposits. For example, minor large clasts with 70-80 mm in diameter were observed ~7 km away from the vent, whereas our simulation predicts that such large clasts are limited near the vent (within 1-2 km). This inconsistency is considered to result from the assumption in our model that the gas-pyroclasts mixture is ejected at the atmospheric pressure with the sound velocity (134 m s^{-1}). On this assumption, the

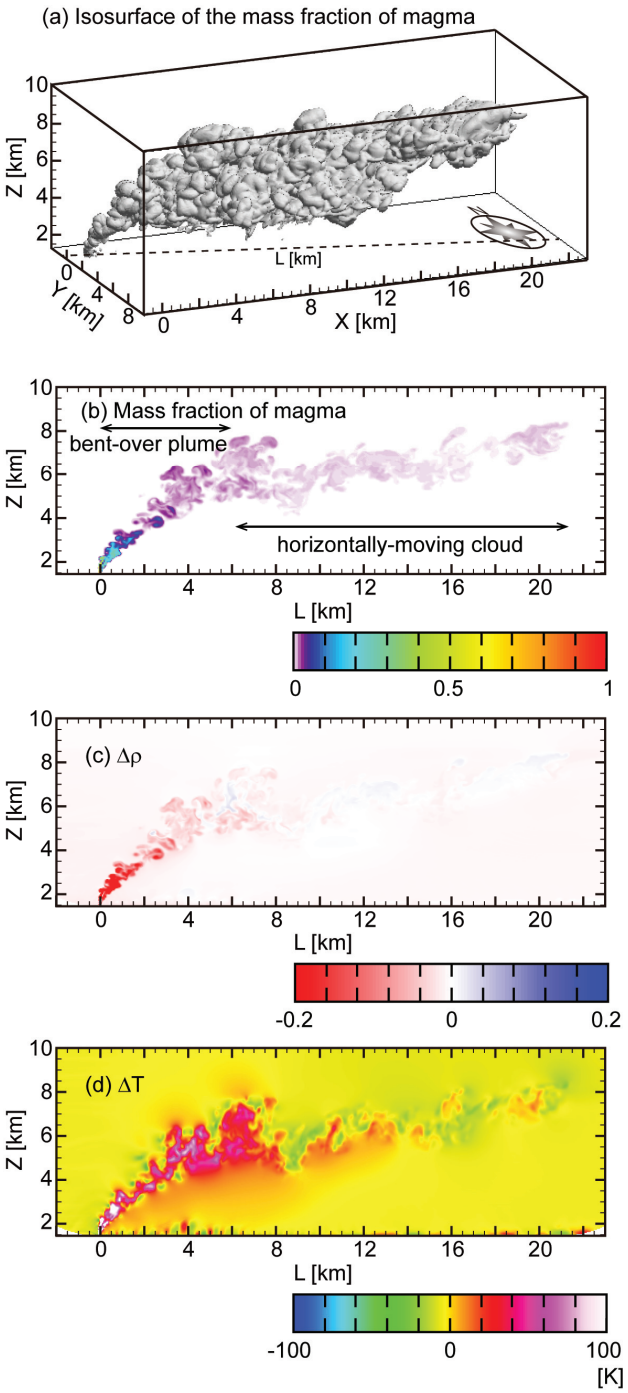

Fig. 2 Results of 3D numerical simulation of a bent-over plume during the 2011 Shinmoe-dake eruptions at 480 s after the eruption. (a) Isosurface of ξ=0.01, where ξ is the mass fraction of the ejected material. Cross-sectional distribution of (b) the mass fraction of the ejected material, (c) density difference relative to stratified atmospheric density at the same vertical height, $\Delta\rho = \rho/\rho_a - 1$, and (d) the temperature difference, $\Delta T = T - T_a$, where T_a is atmospheric temperature. The position of the cross-section is indicated by a dotted line in (a).

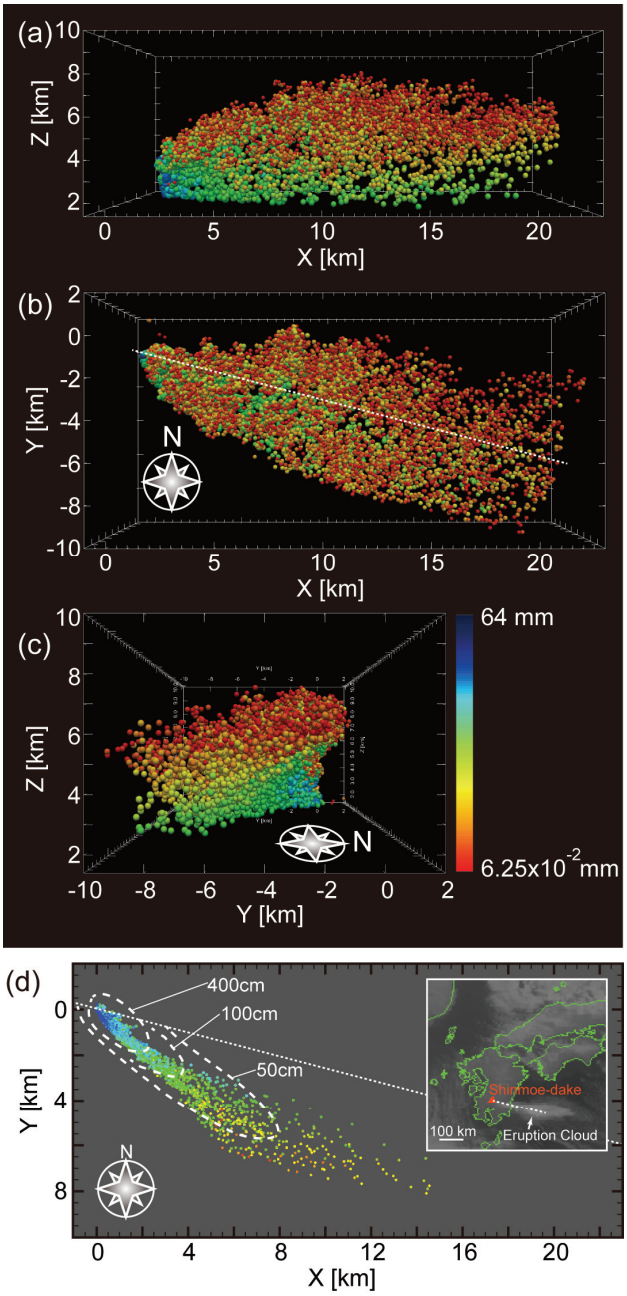

Fig. 3 Distributions of marker particles at 600 s from the eruption. (a) Side view from the south, (b) top view, and (c) side view from the east. (d) Depositional pattern of marker particles at ground level. Particle colors represent particle sizes. The dotted lines in (b) and (d) represent the axis direction of the horizontally moving cloud observed by the satellite image (inset of (d)). The dashed curves in (d) represent isomass lines of the airfall deposits for the 26-27 January 2011 sub-Plinian eruptions of the Shinmoe-dake volcano [13].

large clasts whose terminal velocities are higher than the above exit velocity necessarily leave from the plume at low level and fall to the ground near the vent. On the other hand, in reality, the eruption intensity fluctuates with time and the exit pressure can be higher than the atmospheric pressure. Under these conditions, the flow just above the vent becomes supersonic and transports large clasts up to higher levels [12]. Further studies are needed to evaluate the effects of these processes on column dynamics and tephra dispersal.

References

[1] B. R. Morton, G. Taylor, and J. S. Turner, "Turbulent gravitational convection from maintained and instantaneous sources", Proc. R. Soc. Lond. A, vol.234, pp.1-23, 1956.

[2] R. S. J. Sparks, "The dimensions and dynamics of volcanic eruption columns", Bull. Volcanol, vol.48, pp.3-15, 1986.

[3] C. Bonadonna, J. C. Phillips, and B. F. Houghton, "Modeling tephra sedimentation from a Ruapehu weak plume eruption", J. Geophys. Res., vol.110, B08209, 2005.

[4] M. Bursik, "Effect of wind on the rise height of volcanic plumes", Geophys. Res. Lett., vol.28, no.18, pp.3621-3624, 2001.

[5] T. Shimbori and K. Fukui, "Time variation of the eruption cloud echo height from Shinmoe-dake volcano in 2011 observed by Tanegashima and Fukuoka weather radars: Part II", Rep. Coordinating comm. for Prediction of Volcanic Eruption 109, in Japanese, 2012.

[6] T. Kozono, H. Ueda, T. Ozawa, T. Koyaguchi, E. Fujita, A. Tomiya, and Y. J. Suzuki, "Magma discharge variations during the 2011 eruptions of Shinmoe-dake volcano, Japan, revealed by geodetic and satellite observations", Bull. Volcanol., 75:695, 2013.

[7] Y. J. Suzuki, T. Koyaguchi, M. Ogawa, and I. Hachisu, "A numerical study of turbulent mixing in eruption clouds using a three-dimensional fluid dynamics model", J. Geophys. Res., vol.110, B08201, 2005.

[8] D. Kunii and O. Levenspiel, *"Fluidization Engineering"*, John Wiley, New York, 1969.

[9] Y. J. Suzuki and T. Koyaguchi, "Numerical determination of the efficiency of entrainment in volcanic eruption columns", Geophys. Res.Lett., vol.37, L05302, 2010.

[10] A. Hashimoto, T. Shimbori, and K. Fukui, "Tephra fall simulation for the eruptions at Mt. Shinmoe-dake during 26-27 January 2011 with JMANHM", SOLA, 8, 37-40, 2012.

[11] Y. Suzuki, A. Yasuda, N. Hokanishi, T. Kaneko, S. Nakada, and T. Fujii, "Syneruptive deep magma transfer and shallow magma remobilization during the 2011 eruption of Shinmoe-dake, Japan – Constraints from melt inclutions and phase equilibria experiments, J. Volcanol. Geotherm. Res., vol.257, pp.184-204, 2013.

[12] T. Koyaguchi, Y. J. Suzuki, and T. Kozono, "Effects of the crater on eruption column dynamcis", J. Geophys. Res., vol.115, B07205, 2010.

[13] F. Maeno, M. Nagai, S. Nakada, R. Burden, S. Engwell, Y. Suzuki, and T. Kaneko, "Constraining tephra dispersion and deposition from cyclic subplinean eruptions at Shinmoedake volcano, Kyushu, Japan, 2011", Abst., Japan Geoscience Union Meet., SVC50-07.

火山噴煙の３次元数値シミュレーション：霧島山新燃岳 2011 年噴火の再現

プロジェクト責任者
小屋口剛博　　東京大学　地震研究所
著者
鈴木雄治郎　　東京大学　地震研究所
小屋口剛博　　東京大学　地震研究所

本プロジェクトでは、固体地球と地球表層・大気にまたがる火山現象について、大規模数値シミュレーションを用いた物理過程の理解と計算結果の防災への応用を目指している。特に、火山噴煙の到達高度や火山灰の降灰分布を定量的に正しく再現することに焦点をあて、噴煙ダイナミクスを支配する乱流混合などの素過程の理解を進めている。

爆発的火山噴火における噴煙高度は、単位時間にマグマから大気に供給される熱エネルギーの直接的指標であり、噴火メカニズムや噴火強度を推定する上で貴重な情報源となる。したがって、実際の気象場における噴煙高度と火口での噴出条件を定量的に正しく関係付けることは、火山学上・防災上強く要請されている。そこで、平成 24 年度は、豊富な観測データが得られた新燃岳 2011 年噴火を対象として、3 次元数値シミュレーションによって噴煙高度と火山灰の降灰分布を定量的に再現することを目標とした。

霧島山新燃岳では、2011 年 1 月 26 ～ 27 日に噴煙を形成するサブプリニアン噴火が 3 回発生した。この噴火については、レーダー観測によって噴煙柱が高度 6 ～ 8km まで達したことが明らかにされており（Shimbori and Fukui, 2012）、降下火砕堆積物の分布については詳細な地質調査がなされている（Maeno et al., 2012）。さらに、合成開口レーダー（SAR）による溶岩噴出率データと傾斜変動データを組み合わせた手法によって、火口における噴出率が高精度で決定されている（Kozono et al., 2013）。また、噴火時の霧島火山周辺の気象場については、気象モデルに基づいて計算されている（Hashimoto et al., 2012）。

今年度の研究では、噴煙の非定常 3 次元モデル（Suzuki et al., 2005）を改良し、任意の気象場を初期条件として与えることができるモデルを開発した。新燃岳 2011 年噴火時の山頂周辺の気象場を初期条件として与え、観測によって特定された噴出率を火口での境界条件としてシミュレーションを行なった結果、噴煙の中心軸は風によって大きく曲げられ、6 ～ 8km の高度で水平方向（東南東）へと拡大した。この計算結果はレーダー観測データとよく一致しており、本研究のモデルが、実際の噴煙のダイナミクスを定量的に再現するものであることが検証された。

噴煙の流体計算とともに火山灰粒子を模擬したマーカー粒子の軌跡について計算を行なったところ、細かい粒子は噴煙頂部高度（6 ～ 8 km）に達し、噴煙とともに遠方へと運ばれるが、粗い粒子は火口近傍で噴煙から分離し堆積するという結果が得られた。また、東南東に拡大した噴煙から分離した粒子は、大気下層での北西風に流され、その結果、降下火砕堆積物の分布軸が火口から南東方向へと伸びることが明らかになった。この計算結果は、地質調査によって得られた堆積物の分布軸が、レーダーで観測された噴煙の拡大方向（東南東）からずれて、南東方向に伸びているという観測事実を合理的に説明する。

キーワード:火山噴煙, 火砕流, 降灰分布, 乱流混合, 火山災害